Journal of
Ceramic Science
and Technology

J. Ceram. Sci. Technol. 1-8 (2019)
DOI: 10.4416/JCST2019-00047
available online at: http://www.ceramic-science.com
© 2019 Göller Verlag

Effect of the Evolution of Rheological Behavior over Deagglomeration Time on Optical Transparency of Polycrystalline Alumina Ceramics

A. Rahimian[1], M. Torki[2], S. Ghazanfari[1], B. Movahedi*[2], R. Emadi[1]

[1]Department of Materials Engineering, Isfahan University of Technology, Isfahan 84156 – 83111, Iran
[2]Department of Nanotechnology Engineering, Faculty of Advanced Sciences and Technologies, University of Isfahan, Isfahan, 81746 – 73441, Iran

received June 23, 2019; received in revised form August 6, 2019; accepted August 15, 2019

Abstract

In this study, polycrystalline alumina ceramics were fabricated using slip casting and spark plasma sintering (SPS) methods. After being slip-cast, the samples were sintered at 1 350 and 1 450 °C for 20 min. The effect of the ball-milling time on the rheological behavior of alumina suspensions with different solid loads (65, 70 and 75 wt%) as well as on the ceramic densification process, microstructural evolution and optical transparency was investigated. It was demonstrated that the optimum ball-milling time to obtain rheological behavior suitable for slip casting was 6 h. Those samples prepared in order to demonstrate optimum rheological behavior and sintered at the optimum temperature were transparent. The highest real in-line transmittance (52 % at a wavelength of 640 nm) was determined for those samples ball-milled for 6 h, with 70 wt% solid load and sintered in the SPS process at 1 450 °C.

Keywords: Optical materials, sintering, optical properties, ball milling.

I. Introduction

Transparent alumina ceramics are some of the most important materials used owing to their good mechanical, chemical, thermal and optical properties [1,2]. Tallon *et al.* [3] determined that particles in a size ranging from 100 – 300 nm are best to prepare concentrated suspensions with low viscosity to produce green bodies with sufficiently high green density to full density (99 % theoretical value).

One important factor that can increase the green density of cast samples is the use of a suspension with a relatively high solid load percentage. If the solid load suspensions are stable, casting them will be more successful than casting diluted suspensions. Chemical additives also can optimize the structural arrangement of the particles in the stable suspension [4] so this affects the rheological behaviour of the suspension. Concentrated suspensions affect both ball milling and casting. In addition, higher percentages of solid load are used, the green density increases. It all comes down to choosing the appropriate solid load percentage. If deagglomeration is effective, the maximum green density is increased [5]. Zhang *et al.* [6] investigated the effect of the ball-milling time on the dispersant function. Initially, a suspension of 60 wt% Al_2O_3 with 1.5 wt% polyacrylic sodium (PAA-Na) as a dispersant was subjected to a milling process for 24 h, so the dispersant could cover the Al_2O_3 particles. The optimum milling time resulted in a slurry with low viscosity for slip casting and an average porosity of about 100 nm. However, with high solid loading, it is difficult to achieve a slurry suitable for slip casting. For slurries based on colloidal processing, the milling time plays an important role in the preparation of a ceramic green body with high as-dried density and homogeneity.

The deagglomeration percentage of different solid loads of suspension depends on the conditions. The optimal dispersant was obtained using the diluted suspension after the suspension containing higher solid load percentages was ball-milled [7,8]. If solid load values are higher than 65 % with a stable suspension and low viscosity with near-Newtonian behavior, the casting of these samples produces high as-dried density samples [9,10].

Changes in the morphology of the particles to a spherical form created a stable suspension, compared to other suspensions containing particles with non-spherical morphologies; furthermore, this is a factor that could be responsible for the instability and development of the yield point suspension. This could be due to the relative size distribution of the particles in the center and around the ball milling area [11]. It has been proved that spherical particle morphologies in suspensions with a high solid load percentage are those with the lowest viscosity [12–14].

In alumina ceramics, high transmittance of visible light is obtained by the reduction of light-scattering sources such as pores and large grains. Extremely low porosities (< 0/0.5 %) and small grain sizes (< 1 μm (are essential to obtain highly transparent alumina [15,16]. Lallemant *et al.* [17] have reported that avoiding large agglomerates, narrowing the pore size distribution, reducing the most frequent pore size and avoiding macroscopic heterogeneities within the

* Corresponding author: b.movahedi@ast.ui.ac.ir

green bodies enable high real in-line transmittance (RIT) values to be achieved in the visible and near-infrared spectrum. These ceramics could have become transparent if the residual porosity had been eliminated completely.

In transparent alumina, such microstructural conditions are obtained by sintering at low temperatures in a spark plasma sintering (SPS) process. SPS is an alternative technique for preparing transparent or translucent alumina. To ensure light transmission, the ceramics were fabricated by optimizing the sintering parameters such as pressure, temperature, heating rate, the atmosphere, rheological behavior, and green body preparation. Low heating rates during the SPS process could reduce grain growth and porosity, and increase RIT for the purest alumina [18–21].

The purpose of this study is to study the effects of different ball-milling times on the rheological behavior, densification process and optical transparency and then fabricate optical alumina ceramic using the SPS process. In addition, the grain growth and pore size distribution as well as the microstructure and optical properties were studied in detail.

II. Experimental Procedure

(1) Materials and ceramic processing

Submicron α-alumina powder (Baikowski SAS-France) with a purity of 99.99 %, an average particle size of about 200 nm, and the (BET)-(Micromeritics Instrument Corporation, Japan) specific surface area of about 7.09 m^2/g was used as the raw material. Suspensions were prepared in deionized water (18 MΩ) with different solid load content (65 – 75 wt%) with 0.8 wt% ammonium polyacrylate-Dolapix CE64 (Zschimmer & Schwarz) as the dispersant. The pH was adjusted to 9.5 using NH_4OH. Each suspension was ball-milled for different times (2, 4, 6 and 8 h), the powder-to-ball weight ratio being kept at 1:5. The ball mill speed was selected at 200 rpm. The optimum ball-milling time for different concentrations of alumina and rheological behavior of the suspensions was examined. Jar and balls (10 mm diameter) were made of alumina to prevent impurities in the suspension. An alumina mold (d = 5 cm, h = 3 cm) was used to produce a compact by means of slip casting. The water was sucked from one side of the alumina mold for 48 h and then the wet green bodies were dried at 80 °C for 2 h in an oven. The samples were heated in a SPS process in two cycles of temperature and pressure. The first cycle consisted of 20 min at 1350 °C as the maximum temperature (Fig. 1a), and the second cycle consisted of 20 min at 1450 °C as the maximum temperature (Fig. 1b).

(2) Analysis and characterization methods

The suspension was ball-milled in a high-energy planetary ball mill (Amin Asia Fanavar Pars MPM158). The slurry viscosity was measured with a rotary viscometer (Model LVDV-II; Brookfield, Middleboro, USA) and the rheological behavior was studied. The green densities were determined according to the Archimedes method in deionized water, using wax to prevent water from penetrating the pores in the green bodies. The pore size distribution of the pre-sintered green bodies was monitored by means of mercury porosimetry (Pore Sizer 9320, Micromeritics Instrument Corporation, USA). The real in-line transmittance of the different samples was determined with a spectrophotometer (Model UV3100; SHIMADZU UV-vis-NIR) in the wavelength of 400 – 800 nm. The infrared transmittance of the samples was determined using FTIR (SHIMADZU 8400S) in the wavelength of 2.5 – 7 μm. The samples were polished on both sides to a thickness of 1 mm to measure the RIT and infrared transmittance. The microstructures were observed on the fracture surfaces using scanning electron microscopy (SEM, JEOL 6510). The sintered specimens were cut and polished for thermal etching at 1 100 °C for 10 min to reveal the grain boundaries. At least 200 grains were measured in order to obtain a statistically robust set of data.

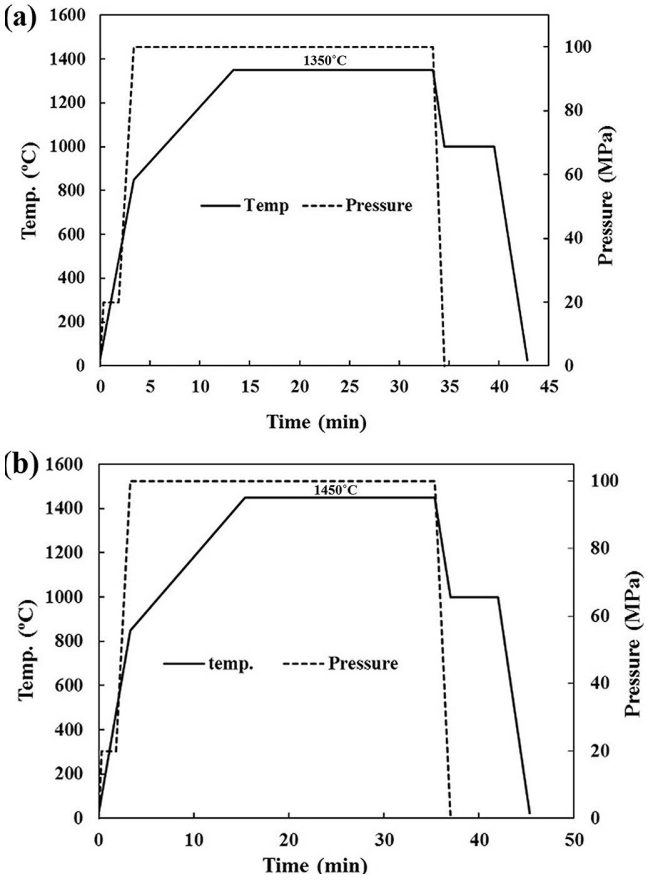

Fig. 1: Graph of the temperature and pressure cycles used in the sintering process of SPS samples at maximum temperature (a) 1 350 °C (b) 1 450 °C.

III. Results and Discussion

(1) Effect of ball milling on rheological behavior

Figs. 2a and 2b show the viscosity and the suspension behavior of three different solid load percentages (65, 70 and 75 wt%) ball-milled for 2 h. The viscosity was increased by increasing the shear rates. This behavior indicated unsuitable conditions and lack of stability owing to the high solid load percentage, agglomeration of the particles and the small amount of free water in the suspension. Shear thickening behavior with thixotropy was observed at all

solid loads. In general, the shear thickening behavior occurred in highly concentrated suspensions with equiaxial particles [12]. The lack of free water in the suspensions caused the formation of a concentrated suspension. In all the suspensions, it was observed with the increase in the solid load, the interactions between particles and viscosity were enhanced [22]. Ball-milling speed in high-viscosity suspensions decreased. So the milling behavior for the different percentages of the solid load could not be the same [23]. As evidenced in Fig. 2, the viscosity was reduced initially in the first hours of ball milling, which was attributed to the breaking up of large, hard and porous agglomerates. The initial agglomerates tend to prevent the exit of water from the channels of pores between the particles. Because of this, less fluid was available to flow. As the hard, large and porous agglomerates were broken up during ball milling, viscosity began to decrease until the particles were well dispersed.

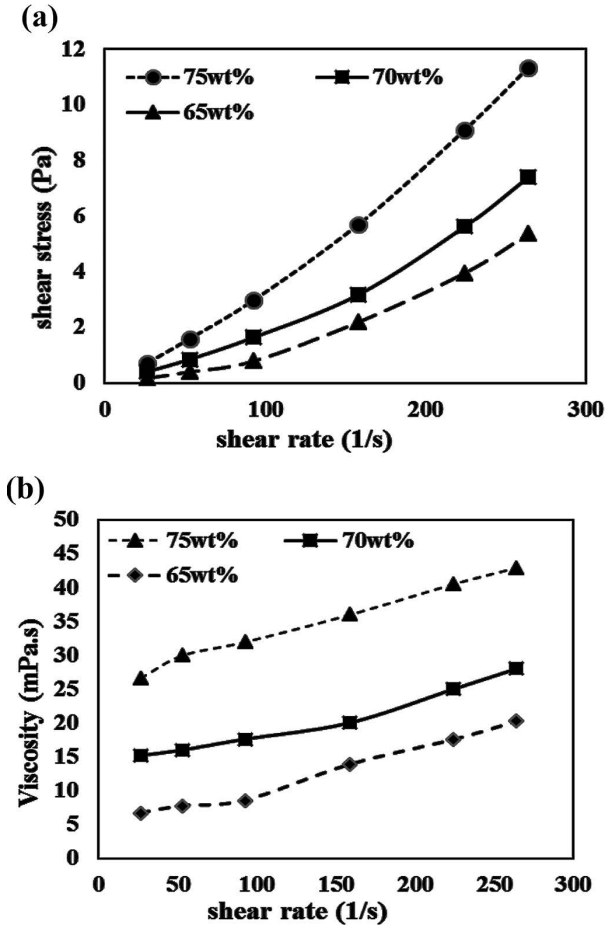

Fig. 2: (a) Changes in the shear stress, (b) Changes in the viscosity of suspensions at different shear rates after 2 h of ball milling.

In Fig. 3, the rheological behavior of the suspensions after 4 h of ball milling is shown. It can be seen that the suspensions with 70 and 75 wt% solid loads are still exhibiting shear thickening behavior and, upon the increase of shear rate, the viscosity increases, as compared with the viscosity values of suspensions after ball milling for 2 h. The reason for this, partial de-agglomeration of particles and the interactions between fine particles was related to the short distances between them; the free water could not leave the pores completely. So, shear thickening behavior was observed [11]. In the case of the suspension containing 65 wt% solid load, after 4 h of ball milling, shear thickening behavior has changed to almost near-Newtonian behavior.

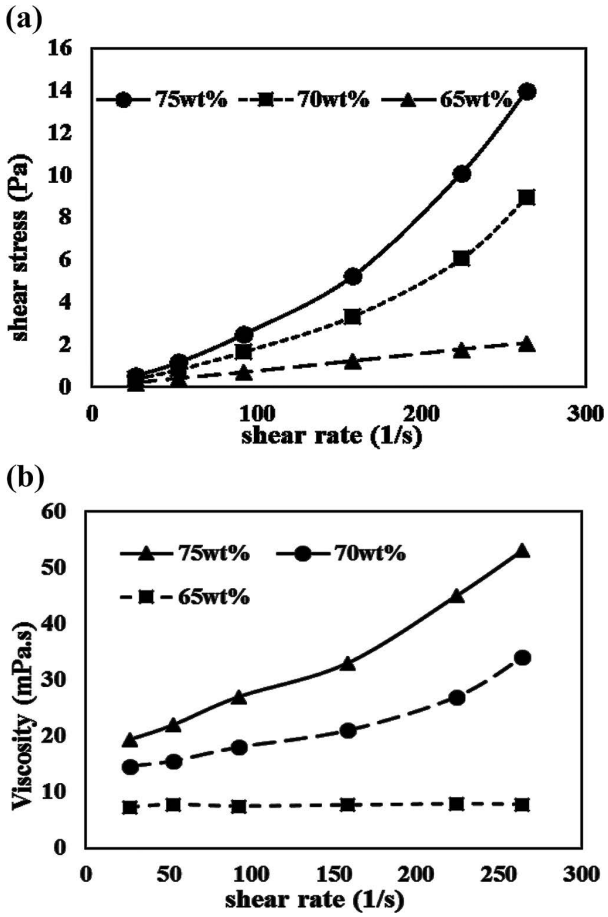

Fig. 3: (a) Changes in the shear stress, (b) Changes in the viscosity of suspensions at different shear rates after 4 h of ball milling.

The rheological behavior of the suspensions after 6 h of ball milling is shown in Figs. 4a and 4b. A significant change in the rheological behavior of the concentrated suspensions was observed. For the suspensions containing 70 and 75 wt% solid loads, the rheological behavior of the suspensions with shear thickening behavior has changed to an almost near-Newtonian behavior. It is probably indicative of the stability of the suspensions, and for the suspension with 65 wt%, shear-thinning rheological behavior with a yield point was observed. It shows that after de-agglomeration, powder particles were broken down. This reduction in particle size increases the interaction between particles and also agglomeration in the concentrated suspension. Driving force is necessary to break up this agglomeration of particles, causing a stress point on the rheology graph [24]. Owing to its shear thinning behavior, with increasing shear rate, large quantities of clots were broken down and increased the viscosity.

Figs. 5a and 5b show the rheological behavior of the suspensions after 8 h of ball milling. It can be seen that in all three suspensions with the different solid load percentages, a change was observed in the state of suspension rheology. Of course, in the case of the suspension with 65 wt% solid load, changes in the rheology behavior have taken place from near-Newtonian to shear thinning

probably owing to the lower viscosity of the suspension with the lower solid load. Subsequently, as expected, with the process of ball milling, two other suspensions (70 and 75 wt% solid loads) have changed from almost near-Newtonian to shear thinning behavior. It should be emphasized that the suspension was de-agglomerated and continued ball milling excessively increased viscosity owing to the instability caused by the changes in the spherical particle morphology and the particles becoming finer. To further confirm this, the changing rheological behavior of the two suspensions with higher solid load subjected to long-time ball milling was analysed. It was shown that the input energy of ball milling for the concentrated suspension, despite the high viscosity, was effective enough to obtain full deagglomeration and change the size and morphology of the particles [25–27].

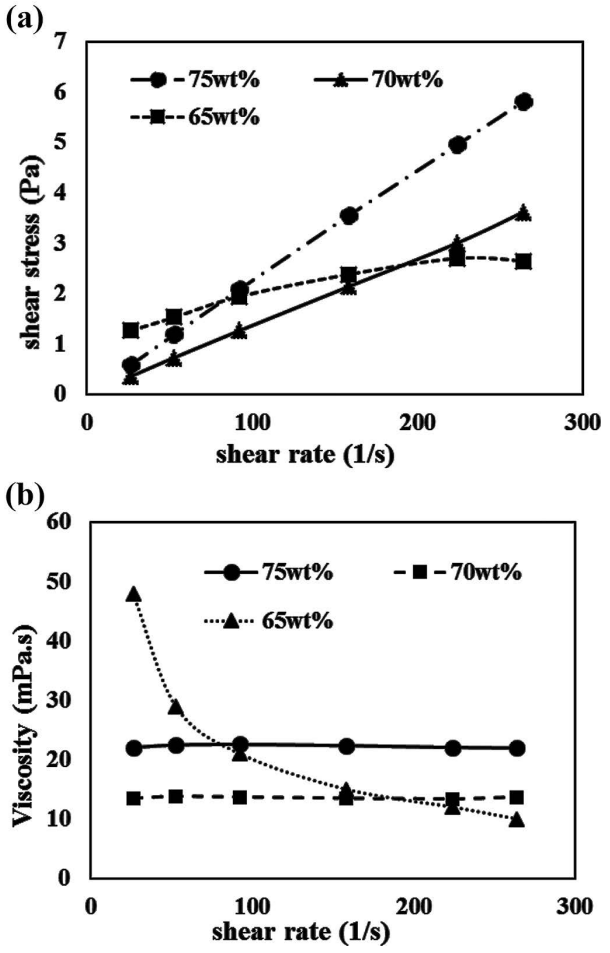

Fig. 4: (a) Changes in the shear stress, (b) Changes in the viscosity of suspensions at different shear rates after 6 h of ball milling.

Ball milling conditions may not be appropriate, and deagglomeration may be incomplete, leading to the change in the particle morphology. Because of the suitable rheological behavior of the suspensions with 70 and 75 wt% solid loads that were ball-milled for 6 h, these were chosen for further investigations with SPS sintering and optical evaluations.

(2) Sintering and microstructural studies

Specifications of the SPS samples are summarized in Table 1. Two samples, S1450 and S75 – 1450, were tested before SPS to determine the pore size and evaluate the effect of the porosity distribution on the transition. Fig. 6 shows the pore size distribution of the two samples S1450 and S75 – 1450. As can be observed, the distribution and porosity volume of the sample S1450 are low. One narrow pore size distribution peak located at 80 nm is obtained by slip casting of deagglomerated alumina powders. The peak is achieved at almost half of the as-received particle size (200 nm), which is an important factor in evaluating slip-cast green bodies [9]. This uniform pore size distribution of slip-cast green body is related to the appropriate morphology of deagglomerated powder and optimized slip casting parameters used for the preparation of the green body. The sample S75 – 1450 had a wider distribution of porosity.

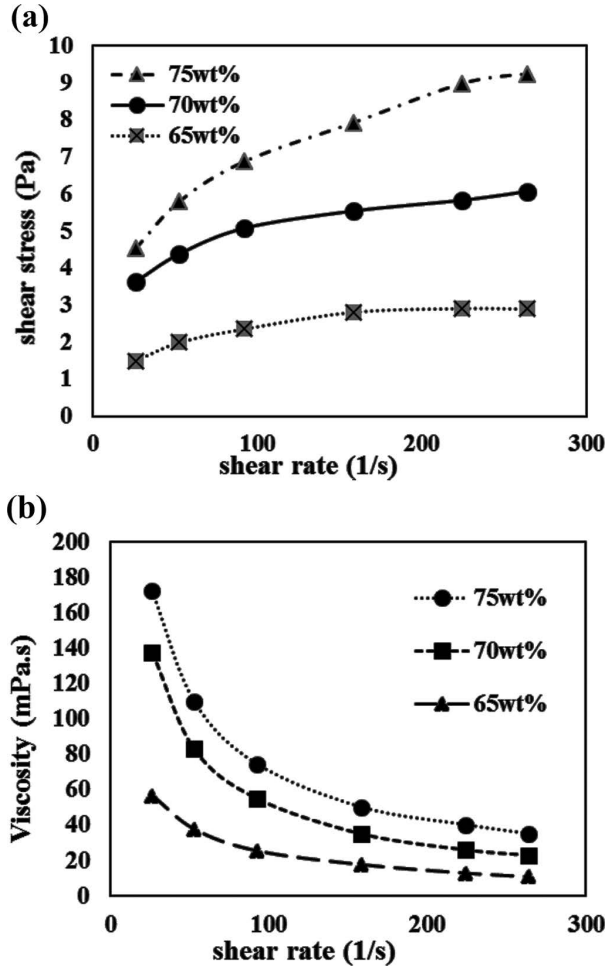

Fig. 5: (a) Changes in the shear stress, (b) Changes in the viscosity of suspensions at different shear rates after 8 h of ball milling.

Fig. 7 shows the polycrystalline alumina ceramics after the SPS process under different conditions. For the SPS samples in this study, the grain size of the optical transparency samples was obtained between 0.8 to 1 μm (Table 1). The reduced grain size of the as-dried density sample (S75 – 1450) could cause the reduction of sintering ability and visible transmittance [28]. Rapid grain growth could occur at sintering temperatures higher than 1 450 °C [29,30]. The green density of the samples was decreased owing to the less stable suspension. In fact, if the primary body is not homogeneous, some residual porosity may not be eliminated. If this porosity cannot be eliminated, the trans-

mittance of the samples is reduced. On the other hand, in this condition, the increase in the sintering temperature only leads to an increase in grain growth and a minor effect on the removed porosity and an increase in the visible and infrared transmittance [24, 31, 32]. Fig. 8 shows the cross-sectional SEM images of the SPS samples. According to these images, intergranular and transgranular porosity was found in S1350 and S75 – 1450 samples, but was not found in the S1450 sample. In addition to controlling grain growth, the use of SPS enabled the fabrication of alumina ceramics with optimum transmittance in the visible region.

(3) RIT and infrared transmission

Fig. 9 presents RIT measurements of the SPS samples. For sample (S1450) fabricated from the suspension with 70 wt% solid load and sintered at 1 450 °C, there was no real in-line transmittance. For the samples made from the optimum suspensions with 70 and 75 wt% solid load with Newtonian behavior, after sintering at 1 450 °C, RIT was determined. As evident in Fig. 9, the real in-line transmission for S1450 at the wavelength of 640 nm reached 52 %. According to the theory of Apetz and Van Bruggen [15], to obtain good RIT in polycrystalline alumina ceramics, as compared with others, we should have a grain size smaller than 250 nm and the relative density should be higher than 99.995 %. Based on this model, RIT depends to an extreme extent on the grain size (light scattering by grains) and porosity. In fact, the level of RIT is very sensitive to residual porosity, grain size and average refractive index changes (Δn) between two adjacent grains. Generally, increasing grain size reduces the amount of RIT (translucent samples) and

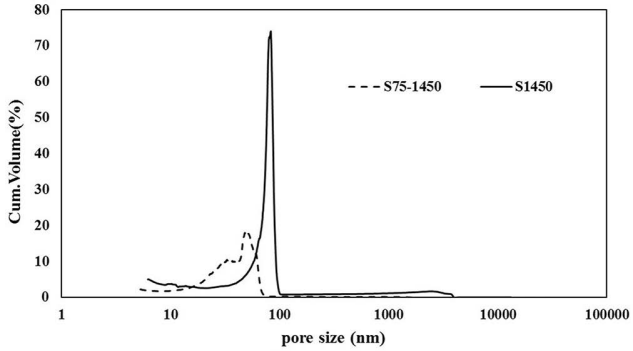

Fig. 6: Pore size distribution of green samples obtained by means of slip casting.

increases porosity, leading to opaque samples (samples are white and milky, Fig. 7, S1350 and S75 – 1450). The sample prepared from the suspension with 70 wt% solid load was in a better condition after the same ball milling time than the suspension of 75 wt% solid load. The higher stability could lead to more homogeneous samples with higher as-dried density. The homogeneity effect of the specified samples could be clearly determined for the sample of 70 wt% solid load after SPS processing at 1 450 °C, as compared to the sample of 75 wt% solid load.

Fig. 10 shows the infrared transmittance of the three samples. Given that some of the samples did not exhibit real in-line transmittance, this graph can help us to better understand the impact of the reduced porosity and the effect of homogeneity on the final microstructure. As can be seen, both S1450 and S75 – 1450 samples showed higher IR than the S1350 sample.

Table 1: Specifications of SPS samples.

Samples	Ball milling time (h)	Solid load (%)	As-dried density (%)	Final SPS temperature (°C)	Average grain growth (μm)	As-sintered density (%)
S1350	6	70	66.7	1 350	0.09±0.94	99.9
S1450	6	70	66.8	1 450	0.06±1.11	99.9
S75 – 1450	6	75	64.5	1 450	0.09±1.13	99.9

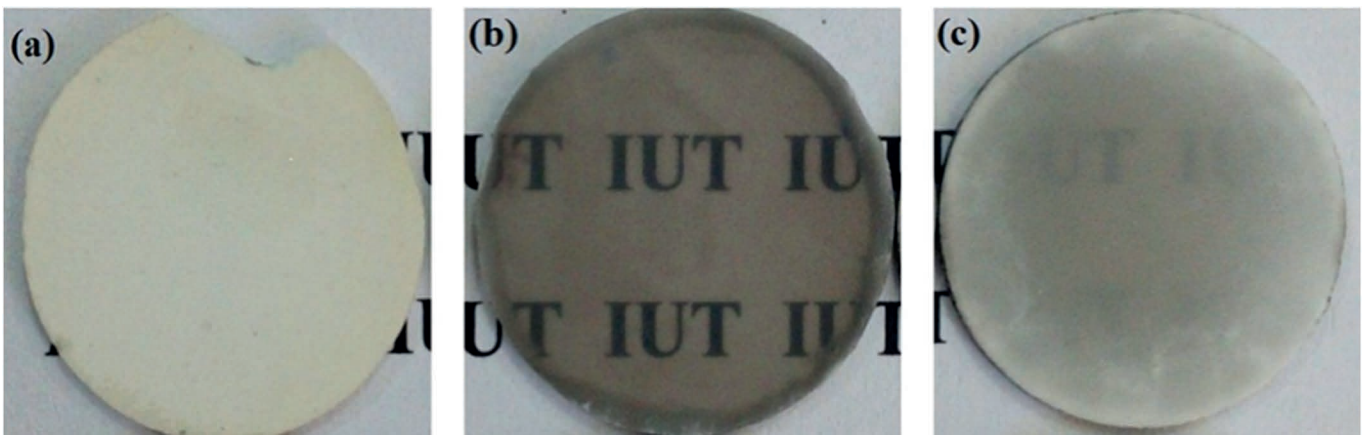

Fig. 7: Polycrystalline alumina ceramics after SPS in different conditions. (a) S1350. (b) S1450 (C) S75 – 1450 samples.

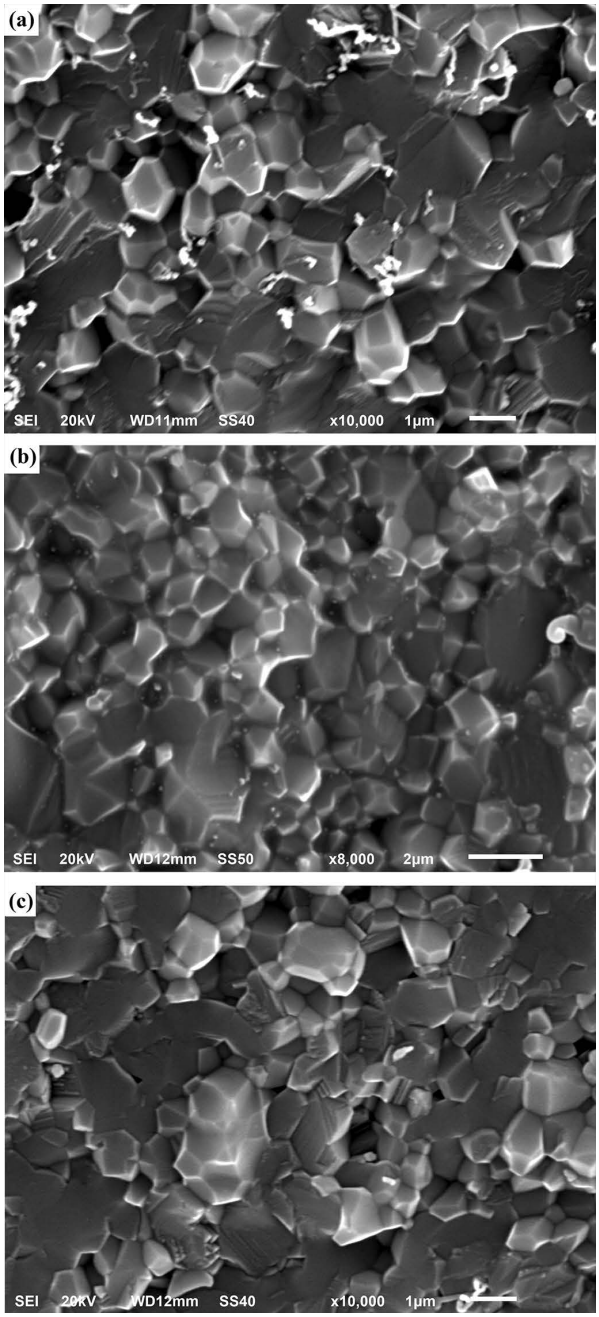

Fig. 8: Cross-sectional SEM images of (a) S1350 (b) S1450 (C) S75 – 1450 samples.

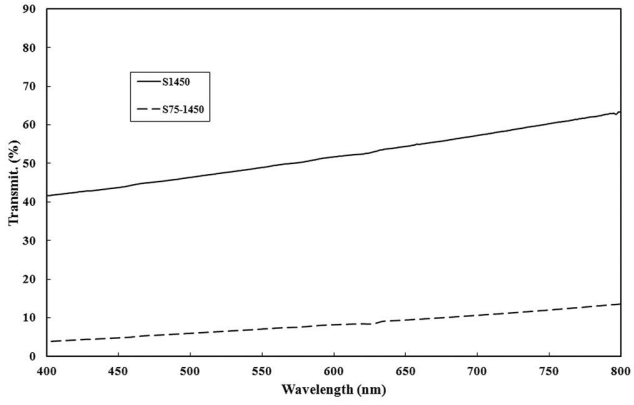

Fig. 9: RIT measurements on 400 – 800 nm wavelength range of slip-cast samples with 70 and 75 wt% solid load after SPS at 1 450°C.

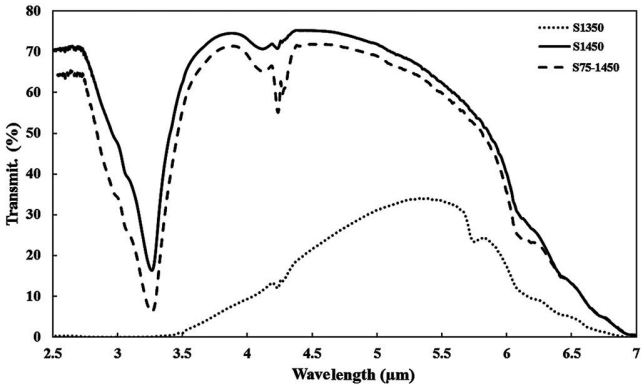

Fig. 10: In-line transmittance of transparent alumina ceramics sintered in the SPS process.

IV. Conclusions

Briefly, it was found that using the different solid load percentages with different ball milling times led to different rheological behavior. The as-dried and as-sintered densities of the specimens obtained with the slip casting method were different. In the case of the suspension with 70 wt% solid load and 6 h of ball milling, the best milling behavior was observed. With this suspension, the samples were obtained with the as-dried density of 67 %. This density was the highest primary density observed compared with all the other samples. The optimized suspension with 70 wt% solid load was sintered in the SPS process for 20 min at 1 450 °C, and exhibited the highest RIT of all the samples. In this case, the real in-line transmission at the wavelength of 640 nm reached 52 %. The infrared transmittance of this sample was higher than that of all other samples, reaching 75 % at the wavelength of 4.5 μm.

References

1 Krell, A., Klimke, J., Hutzler, T.: Advanced spinel and sub-μm Al_2O_3 for transparent armour applications, *J. Eur. Ceram. Soc.*, **29**, 275 – 281, (2009).

2 Krell, A., Hutzler, T., Klimke, J.: Transmission physics and consequences for materials selection, manufacturing, and applications, *J. Eur. Ceram. Soc.*, **29**, 207 – 221, (2009).

3 Tallon, C., Limacher, M., Franks, G.V. Effect of particle size on the shaping of ceramics by slip casting, *J. Eur. Ceram. Soc.*, **30**, 2819 – 2826, (2010).

4 Kafili, G., Loghman-Estarki, M.R., Milani, M., Movahedi, B. The effects of TEOS on the microstructure and phase evolutions of YAG phase by formation of alumina/yttria core-shell structures, *J. Am. Ceram. Soc.*, **100**, 4305 – 4316, (2017).

5 Dhara, S., Bhargava, P.: Influence of Slurry Characteristics on Porosity and Mechanical Properties of Alumina Foams, *Int. J. Appl. Ceram. Technol.*, **3**, 382 – 392, (2006).

6 Sokol, M., Kalabukhov, S., Kasiyan, V., Rothman, A., Dariel, M.P., Frage, N.: Mechanical, thermal and optical properties of the SPS-processed polycrystalline Nd:YAG, *Opt. Mater.*, **38**, 204 – 210, (2014).

7 He, M., Wang, Y., Forssberg, E.: Slurry rheology in wet ultrafine grinding of industrial minerals: A review, *Powder technol.*, **147**, 94 – 112, (2004).

8 Stuer, M., Bowen, P.: Yield stress modelling of doped alumina suspensions for applications in freeze granulation: towards dry pressed transparent ceramics, *Adv. Appl. Ceram.*, **111**, 254 – 261, (2012).

9 Krell, A., Klimke, J.: Effects of the homogeneity of particle coordination on solid state sintering of transparent alumina, *J. Am. Ceram. Soc.*, **89**, 1985 – 1992, (2006).

10 Thiele, E.S., Setter, N.: Lead zirconate titanate particle dispersion in thick- film ink formulations, *J. Am. Ceram. Soc.*, **83**, 1407 – 1412, (2000).

11 Farrokhpay, S.: The importance of rheology in mineral flotation: A review, *Miner. Eng.*, **36**, 272 – 278, (2012).

12 Rahaman, M.N.: Ceramic processing. Wiley Online Library, 2006.

13 Klement, R., Rols, S., Mikulikova, R., Krestan, J.: Transparent armour materials, *J. Eur. Ceram. Soc.*, **29**, 275 – 281, (2009).

14 Takao, Y., Hotta, T., Naito, M., Shinohara, N., Okumiya, M., Uematsu, K.: Microstructure of alumina compact body made by slip casting, *J. Eur. Ceram. Soc.*, **22**, 397 – 401, (2002).

15 Apetz, R., van Bruggen, M.P.B.: Transparent Alumina: A light-scattering model, *J. Am. Ceram. Soc.*, **86**, 480 – 486, (2003).

16 Eftekhari, A., Movahedi, B., Dini, G., Milani, M.: Fabrication and microstructural characterization of the novel optical ceramic consisting of α-Al_2O_3@ amorphous alumina nanocomposite core/shell structure, *J. Eur. Ceram. Soc.*, **38**, 3297 – 3304, (2018).

17 Lallemant, L., Fantozzi, G., Garnier, V., Bonnefont, G.: Transparent polycrystalline alumina obtained by SPS: green bodies processing effect, *J. Eur. Ceram. Soc.*, **32**, 2909 – 2915, (2012).

18 Kafili, G., Movahedi, B., Milani, M.: A comparative approach to synthesis and sintering of alumina/yttria nanocomposite powders using different precipitants, *Mater. Chem. Phys.*, **183**, 136 – 144, (2016).

19 Jiang, D.T., Hulbert, D.M., Anselmi-Tamburini, U., Ng, T., Land, D., Mukherjee A.K.: Optically transparent polycrystalline Al_2O_3 produced by spark plasma sintering, *J. Am. Ceram. Soc.*, 91, 151 – 154, (2008).

20 Kim, B.-N., Hiraga, K., Morita, K., Yoshida, H.: Effects of heating rate on microstructure and transparency of spark-plasma-sintered alumina, *J. Eur. Ceram. Soc.*, **29**, 323 – 327, (2009).

21 Kim, B-N., Hiraga, K., Morita. K., Yoshida, H., Miyazaki, T., Kagawa, Y.: Microstructure and optical properties of transparent alumina, *Acta Mater.*, **57**, 1319 – 1326, (2009).

22 Mohammadi, F., Mirzaee, O., Tajally, M.: Influence of solid loading on the rheological, porosity distribution, optical and the microstructural properties of YAG transparent ceramic, *Ceram. Int.*, **44**, 12098 – 12105, (2018).

23 Stenger, F., Peukert, W.: The role of particle interactions on suspension rheology-application to submicron grinding in stirred ball mills, *Chem. Eng. Technol.*, **26**, 177 – 183, (2003).

24 Shafeiey, A., Enayati, M.H., Al-Haji, A.: The effect of slip casting parameters on the green density of $MgAl_2O_4$ spinel, *Ceram. Int.*, **43**, 6069 – 6074, (2017).

25 Bowen, P., Carry, C., Luxembourg, D., Hofmann, H.: Colloidical proccessing and sintering of nonosized transition aluminas, *Powder Technol.*, **157**, 100 – 107, (2005).

26 Liu, J., Lin, L., Li, J., Liu, J., Yuan, Y., Ivanov, M., Chen, M., Liu, B., Ge, L., Xie, T.: Effects of ball milling time on microstructure evolution and optical transparency of Nd: YAG ceramics, *Ceram. Int.*, **40**, 9841 – 9851, (2014).

27 Lange, F.F., Yul. B.C.: Shape forming alumina slurries via colloidal isopressing, *J. Eur. Ceram. Soc.*, **30**, 2795 – 2803, (2010).

28 Xue, L.A., Chen, I.: Deformation and grain growth of low temperature sintered high purity alumina, *J. Am. Ceram. Soc.*, **73**, 3518 – 3521, (1990).

29 Li, J., Ye, Y.: Densification and grain growth of Al_2O_3 nanoceramics during pressureless sintering, *J. Am. Ceram. Soc.*, **89**, 139 – 143, (2006).

30 Galusek, D., Sedláček, J., Chovanec, J., Michálková, M.: The influence of MgO, Y_2O_3 and ZrO_2 additions on densification and grain growth of submicrometre alumina sintered by SPS and HIP, *Ceram. Int.*, **41**, 9692 – 9700, (2015).

31 Queiroga, J.A., Nunes, E.H.M., Souza, D.F., Vasconcelos, D.C.L., Ciminelli, V.S.T., Vasconcelos, W.L.: Microstructural investigation and performance evaluation of slip-cast alumina supports, *Ceram. Int.*, **43**, 3824 – 3830, (2017).

32 Yang, J., Oliveira, F.J., Ferreira, J.M.F.: Pressureless sintering of slip cast silicon nitride bodies prepared from coprecipitation coated powders, *J. Eur. Ceram. Soc.*, **19**, 433 – 439, (1999).